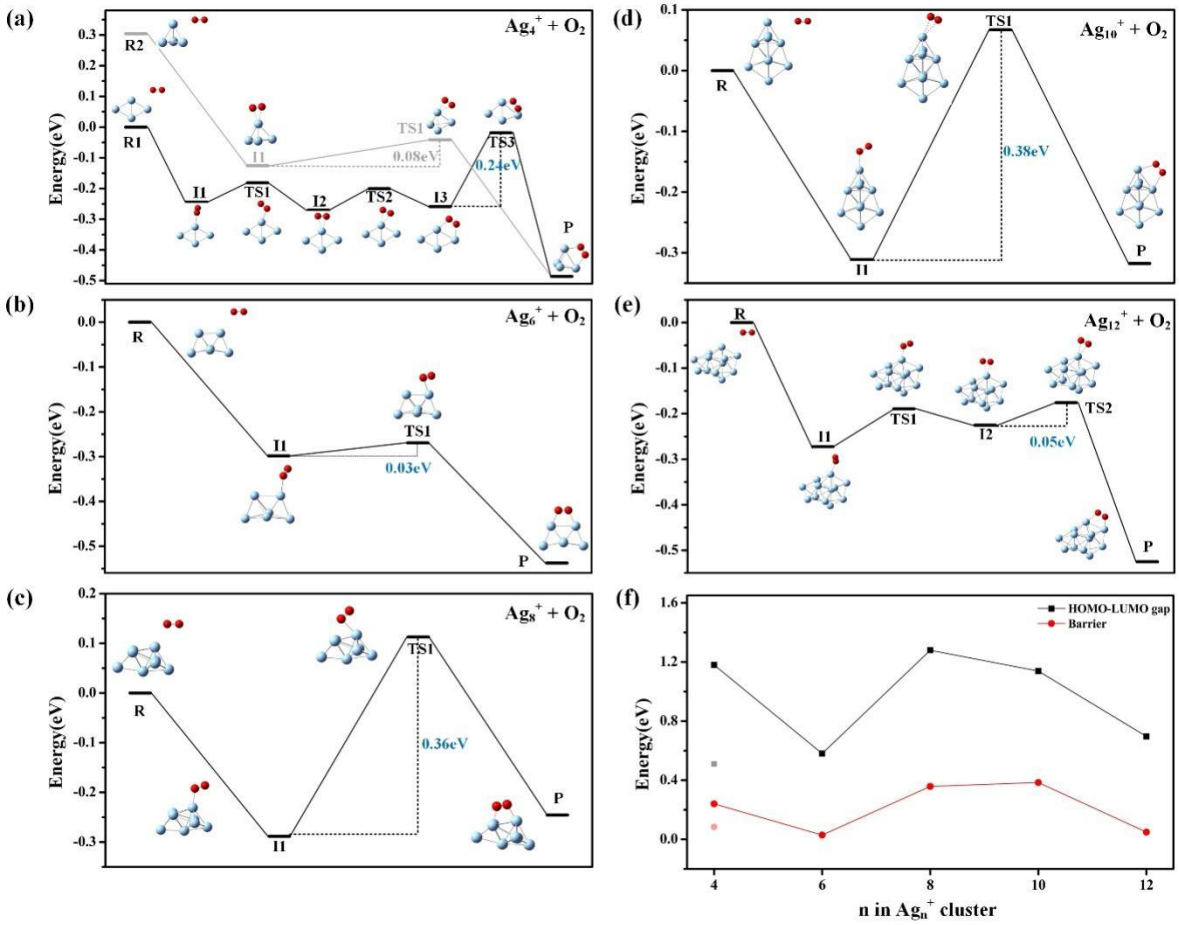

Figure S11. The reaction paths of the dominant structures of Ag_n^+ (n = 4, 6, 8, 10, 12) with O_2 (a-e) and the comparisons between their barriers from the physisorbed O_2 to the chemisorbed O_2 and their HOMO-LUMO gaps. The gray lines in (a) and the gray points in (f) show the results of the pyramid isomer of Ag_4^+.

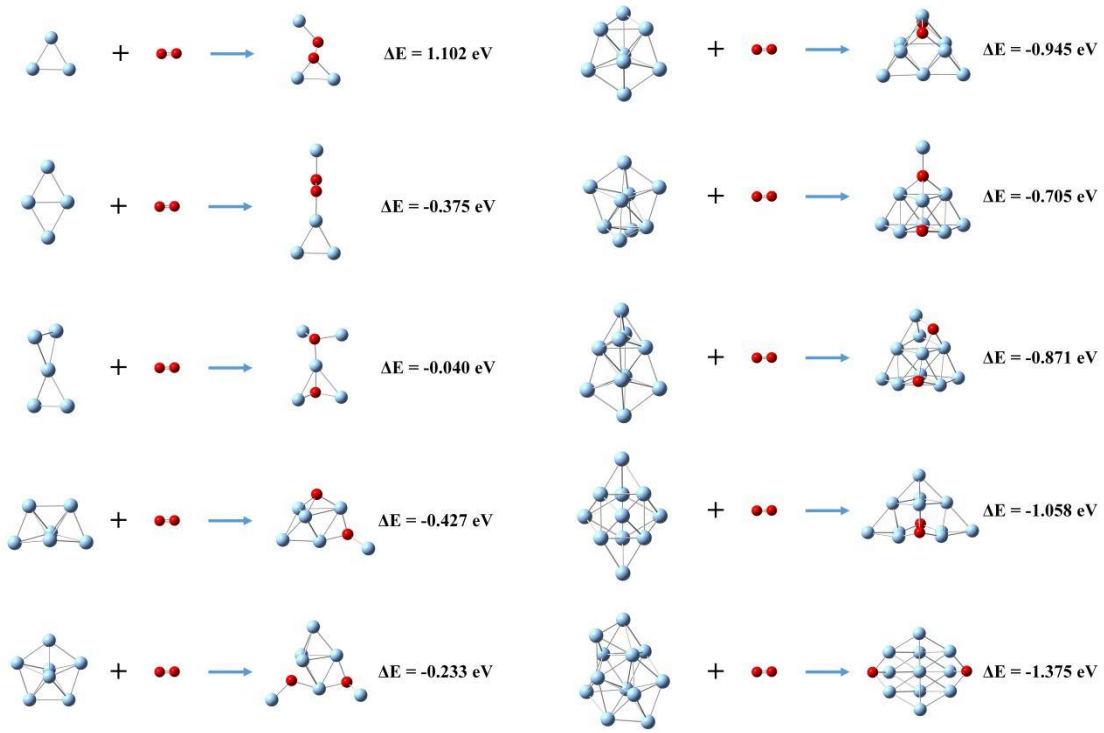

Figure S12. The lowest lying structures of $Ag_nO_2^+$ (n = 3-12) with O_2 inserted into or dissociated on the silver moiety and their energies relative to the initial reactants Ag_n^+ and O_2.

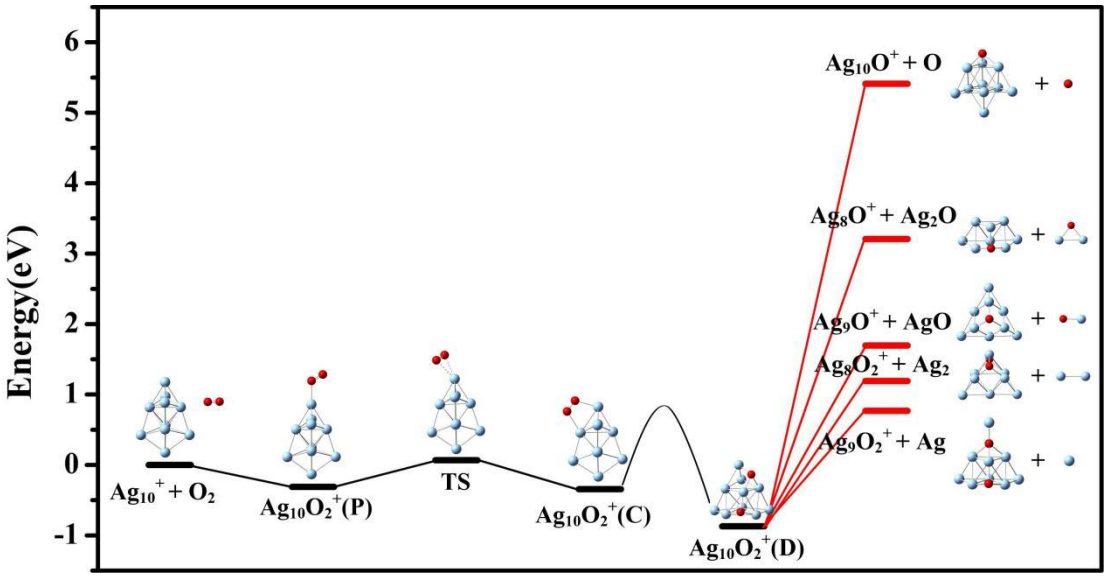

Figure S13. The relative energies of the reaction products between Ag_{10}^{+} with O_2 including those of the physisorption, the chemisorption, the dissociation, and the etching steps.

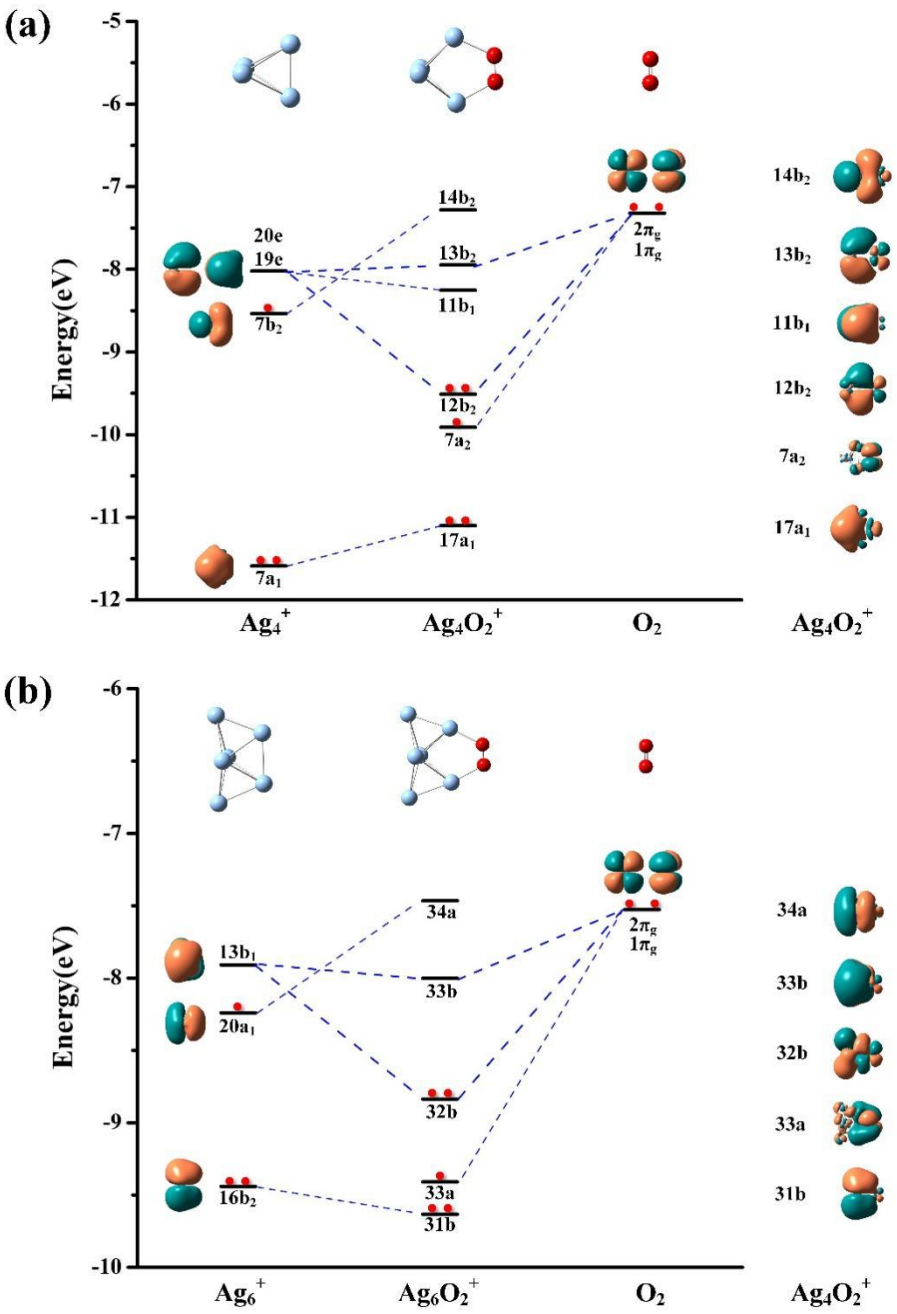

Figure S14. The bonding scheme of $Ag_4O_2^+$(a) and $Ag_6O_2^+$(b), illustrating the bonding interactions between the bare cluster $Ag_{4/6}^+$ and the O_2 fragment as well as their canonical Kohn–Sham frontier valence MOs (isosurface = 0.01 a.u.).